Quantitative imaging of the Dorsal nuclear gradient reveals limitations to threshold-dependent patterning in *Drosophila*

Louisa M. Liberman[1], Gregory T. Reeves[1], and Angelike Stathopoulos[2]

Division of Biology, California Institute of Technology, 1200 East California Boulevard, MC114-96, Pasadena, CA 91125

Edited by Eric H. Davidson, California Institute of Technology, Pasadena, CA, and approved November 3, 2009 (received for review June 4, 2009)

The NF-κB-related transcription factor, Dorsal, forms a nuclear concentration gradient in the early *Drosophila* embryo, patterning the dorsal-ventral (DV) axis to specify mesoderm, neurogenic ectoderm, and dorsal ectoderm cell fates. The concentration of nuclear Dorsal is thought to determine these patterning events; however, the levels of nuclear Dorsal have not been quantified previously. Furthermore, existing models of Dorsal-dependent germ layer specification and patterning consider steady-state levels of Dorsal relative to target gene expression patterns, yet both Dorsal gradient formation and gene expression are dynamic. We devised a quantitative imaging method to measure the Dorsal nuclear gradient while simultaneously examining Dorsal target gene expression along the DV axis. Unlike observations from other insects such as *Tribolium*, we find the Dorsal gradient maintains a constant bell-shaped distribution during embryogenesis. We also find that some classical Dorsal target genes are located outside the region of graded Dorsal nuclear localization, raising the question of whether these genes are direct Dorsal targets. Additionally, we show that Dorsal levels change in time during embryogenesis such that a steady state is not reached. These results suggest that the multiple gene expression outputs observed along the DV axis do not simply reflect a steady-state Dorsal nuclear gradient. Instead, we propose that the Dorsal gradient supplies positional information throughout nuclear cycles 10-14, providing additional evidence for the idea that compensatory combinatorial interactions between Dorsal and other factors effect differential gene expression along the DV axis.

development | gene expression

The morphogen gradient model describes how positional information is conferred to a field of cells, enabling the specification of different cell types. In this model, a diffusible molecule forms a concentration gradient that dictates differential gene expression in a concentration dependent fashion. Appealing in its simplicity, this concept has been used to explain cell-fate specification and patterning in animals (1).

The NF-κB homolog, Dorsal, is present in a nuclear concentration gradient within the *Drosophila melanogaster* embryo (reviewed in ref. 2). The asymmetries that result in the Dorsal gradient are initialized in the egg before fertilization by Gurken-dependent signaling. After fertilization, this DV information is relayed to the embryo through ventrally localized maturation of the Toll-receptor ligand, Spätzle. Toll activation directs the degradation of the IκB homolog, Cactus, allowing Dorsal to enter the nucleus. Although the maternally deposited *dorsal* mRNA and the translated protein are initially uniform within the early embryo, nuclear import of Dorsal selectively occurs in ventral regions as a result of Toll activation, resulting in a nuclear concentration gradient that is first visible at nuclear cycle (nc) 10, when nuclei migrate to the periphery of the embryo. Using transgenic flies with a Dorsal-GFP fusion protein, it has been observed that Dorsal shuttles continuously between the nucleus and the cytoplasm of precellularized embryos (3). This shuttling occurs during each interphase of nc 10–14 and occurs in all of the nuclei—including those located in dorsal regions.

Dorsal is required for patterning the germ layers along the DV axis, functioning as both an activator and a repressor of transcription (reviewed in ref. 4). In ventral regions where Dorsal concentration is high, Dorsal positively regulates the expression of the genes *twist* and *snail* to specify the presumptive mesoderm. Lower levels of Dorsal in lateral regions activate the expression of genes in the presumptive neurogenic ectoderm, including *rhomboid* (*rho*), *brinker* (*brk*), *intermediate neuroblasts defective* (*ind*), and *short gastrulation* (*sog*). In contrast, Dorsal functions as a repressor of presumptive dorsal ectoderm genes, such as *zerknüllt* (*zen*) and *decapentaplegic* (*dpp*), restricting their expression to dorsal regions where Dorsal protein levels are lowest. The predominant model proposes that Dorsal binds to regulatory regions of target genes with differential affinity resulting in gene expression that is dependent upon the nuclear Dorsal concentration (5–7). However, Dorsal does not function alone to regulate the expression of genes: affinity of binding sites is influential but combinatorial interactions with other transcription factors are also thought to be important (e.g., refs. 8–10).

We propose that nuclear Dorsal levels must be measured to determine the role Dorsal plays to direct distinct gene expression outputs. The requirement of the Dorsal gradient for patterning the DV axis has received much attention, although few groups have attempted to quantify the levels of Dorsal in the embryo (11) and none have specifically measured nuclear levels. Here we develop a method to measure nuclear Dorsal levels during nc 10–14 of fixed embryos. This approach has two advantages over live imaging: first, we can simultaneously observe both Dorsal protein levels and gene expression, and secondly, we can obtain a larger data set to observe variability that may exist at a given developmental stage. We used wild-type (wt) and mutant embryos with genetically manipulated levels of nuclear Dorsal to ask whether nuclear Dorsal protein can be used to predict gene expression outputs. We conclude that a steady dose of Dorsal does not determine gene expression boundaries, as predicted by the classical morphogen paradigm. Instead, our data support a model in which temporal dynamics as well as combinatorial interactions with other factors must be considered to understand DV patterning.

Results

The Dorsal nuclear gradient supplies positional information to the DV axis in developing *Drosophila* embryos, yet the levels of

Author contributions: L.M.L. and A.S. designed research; L.M.L. and G.T.R. performed research; L.M.L. and G.T.R. analyzed data; and L.M.L., G.T.R., and A.S. wrote the paper.

The authors declare no conflict of interest.

This article is a PNAS Direct Submission.

[1]L.M.L and G.T.R contributed equally to this work.

[2]To whom correspondence should be addressed. E-mail: angelike@caltech.edu.

This article contains supporting information online at www.pnas.org/cgi/content/full/0906227106/DCSupplemental.

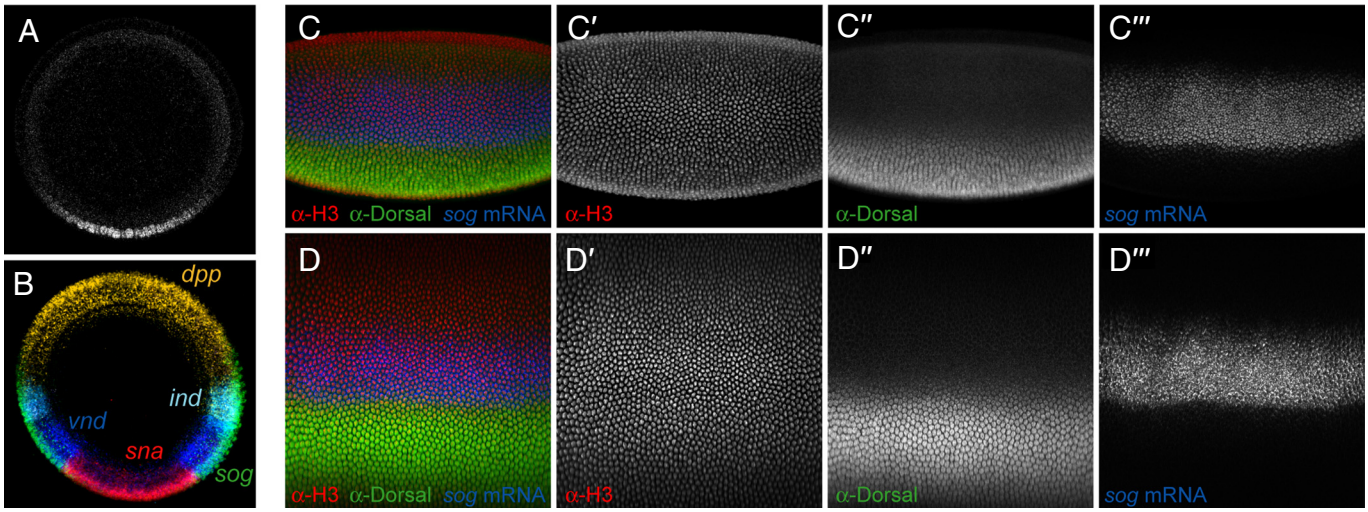

Fig. 1. Cross-sections and whole mount in situ hybridizations and antibody staining. (*A*) Dorsal antibody staining visualized by manual cross-section. (*B*) mRNA in situ hybridization of genes expressed along the DV axis. (*C*) Three-dimensional whole mount in situ hybridization of *sog* gene expression in a single embryo, shown in blue, detected using a riboprobe made to the *sog* transcript, co-labeled using antibodies for Dorsal protein (green) and Histone H3 (red). (*D*) Computational unrolling of 3D images of whole mount embryo from *C* allows for protein and mRNA expression to be analyzed in 2D. This technique was used to generate the quantitative data for each of the following figures. [*A* and *B* reproduced with permission from Reeves GT, Stathopoulos A (Graded Dorsal and differential gene regulation in the *Drosophila* embryo. *Perspectives on Generation and Interpretation of Morphogen Gradients*, eds Briscoe J, Lawrence P, Vincent J.-P. (Copyright 2009, Cold Spring Harbor Lab Press, Plainview, NY).]

nuclear Dorsal relative to target gene expression domains have not been defined. To this end, we performed antibody staining to view Dorsal and Histone proteins, while gene expression was observed by in situ hybridization. This approach allowed us to quantify nuclear Dorsal concentrations across the embryo and compare these levels with expression patterns of select target genes in the neurogenic ectoderm (Fig. 1 *A* and *B*; see *SI Text*).

We collected three-dimensional (3D) stacks of confocal microscope images of embryos at nc 10–14 (Fig. 1*C*). We computationally unrolled images (see *Materials and Methods* and *SI Text*, section 1) (12) to produce a two-dimensional (2D) picture of a 3D embryo (Fig. 1*D*). At this stage, all of the nuclei have migrated to the periphery of the embryo, and thus these 2D representations allow for simplified segmentation and data analysis (Fig. 1, histone levels: *C′* and *D′*, Dorsal concentration: *C″* and *D″*, and *sog* gene expression: *C‴* and *D‴*).

We find that the distribution of nuclear Dorsal at all stages is roughly bell-shaped, and thus can be empirically fit to a Gaussian curve (see Fig. 2 *A*–*C*, *Materials and Methods*, and *SI Text*, section 6). In ventral–lateral regions of the embryo, where *vnd* expression and the ventral portion of *sog* expression are observed (Fig. 2 *A* and *B*), the nuclear localization of Dorsal decreases sharply, consistent with previous studies (13–15). However, in intermediate regions of the embryo, where *ind* and the dorsal portions of *sog* and *brk* are expressed, and where the borders of dorsally localized genes such as *dpp* and *zen* are positioned, nuclear Dorsal protein levels decrease to the same basal levels observed in dorsal-most regions of the embryo (Fig. 2 *B* and *C*). In particular, the bulk of *ind* expression is almost always seen in the regions where Dorsal is at basal levels, outside of the graded distribution of Dorsal (Fig. 2*C*). We find that nuclear Dorsal reaches basal levels at approximately 110 μm from the ventral midline (Fig. 2 *C* and *D*).

It is important to note that these basal levels correspond to a non-zero concentration of nuclear Dorsal. The Dorsal antibody has some low level of non-specific background staining, assayed by imaging embryos derived from homozygous dl^1/dl^1 mothers, which produce no Dorsal protein (13). However, nuclear Dorsal levels detected in wt embryos exceed this dl^1 background staining, even in the dorsal-most regions of the embryo (Fig. 2). For the remainder of the paper, "basal levels" of Dorsal refer to the non-zero levels of nuclear Dorsal achieved in the dorsal portion of the embryo, and all subsequent gradients are plotted with the dl^1 background subtracted.

Considering these observations, we asked whether the Dorsal gradient is initially broad and later refines. If a transient exposure to Dorsal supports gene expression, this could explain how positional information is supplied to intermediate regions to establish the expression boundaries of genes such as *ind* and *sog*. However, plotting normalized Dorsal gradients reveals a constant gradient width throughout all nuclear cycles (Fig. 3*C*). To quantify this observation, we used the empirically fit Gaussian parameters, finding the variation in gradient widths to be 16% (standard deviation divided by the mean), which we attribute to natural variation. For comparison, variation in embryo sizes used in this study was similar, at 15%. Furthermore, when grouped by nuclear cycle, the gradient widths are not significantly different from one another (Fig. 3*D* and *SI Text*, section 13).

In contrast to the consistency of gradient widths, nuclear Dorsal levels vary significantly during each nuclear cycle (Fig. 3*A*). We propose that this variability is due to the dynamics of the nuclear cycles and the nuclear accumulation of Dorsal. During mitosis, the nuclei break down, forcing Dorsal and other nuclear factors into the cytoplasm (13, 16). We surmise that, following each nuclear division, Dorsal begins to accumulate in the nuclei, and as interphase proceeds, the concentration of nuclear Dorsal changes in time according to import/export rates as well as nuclear shape changes (16). Therefore, our data reflect that we are observing different instances of a dynamic process. This is consistent with previous work showing that Dorsal protein localization during gradient formation is dynamic, but tends to increase during a single nuclear cycle (3). To test our hypothesis, we conducted a detailed analysis of nc 14 embryos, showing a correlation between Dorsal levels and age within nc 14 (*SI Text*, section 8).

In addition to these observations, we identified two new trends in these data. The average Dorsal levels in the ventral-most nuclei increase from nc 10–14; on the other hand, the average basal levels of Dorsal decrease over this same period (Fig. 3 *A Inset* and *B*). These trends are statistically significant

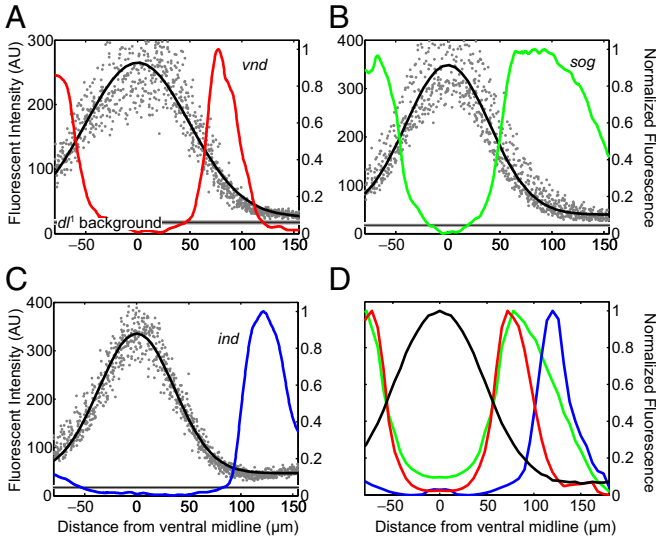

Fig. 2. Dorsal quantification and target mRNA expression in individual wt embryos shows the location of germ layer-specific target gene expression at nc 14. (*A*–*C*) Single embryo measurements of fluorescent intensity values of Dorsal within the nuclei (gray dots) fit by best-fit Gaussian curves (black curve) in raw fluorescent intensity units (left axis). Colored curves represent normalized intensity of gene expression (right axis). Numbers on the *x* axis represent distance from the ventral midline. dl^1/dl^1 mutants were used to determine background fluorescence in the absence of Dorsal protein (horizontal black line; standard deviation shown as thickness of line). (*A*) *vnd* expression (red trace) starts within the steepest part of the Dorsal gradient and ends at the dorsal border of Dorsal nuclear localization. (*B*) *sog* expression (green trace) spans from the ventral region of *vnd* expression to lateral regions of the embryo where Dorsal levels are uniform. (*C*) *ind* expression (blue trace) lies largely outside the Dorsal gradient. Note that the amplitudes of Dorsal concentration vary among the three embryos shown; this variability is seen even when the embryos are all at the same nuclear cycle (see Fig. 3). (*D*) Overlay of all three gene expression outputs (averages of multiple embryos; $n = 12$ for *vnd*, 7 for *sog*, and 8 for *ind*) onto a single plot with averaged Dorsal gradient in black ($n = 35$ nc 14 embryos).

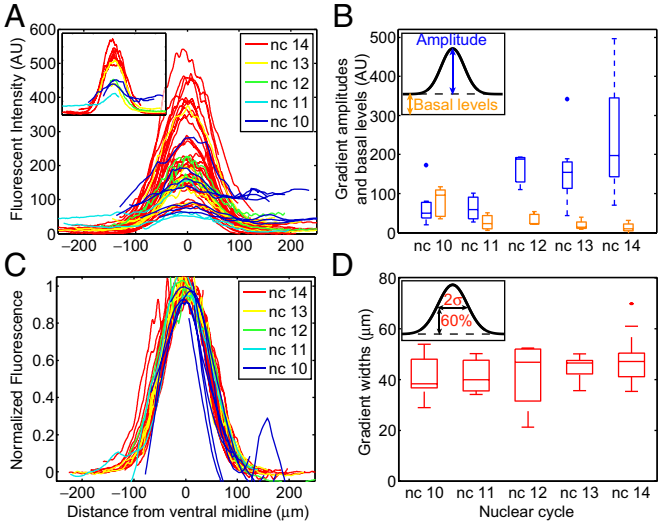

Fig. 3. Developmental time course of wt Dorsal gradient shows no change in the width of the gradient centered at the ventral midline. (*A*) Whole mount quantification of Dorsal levels in computationally staged embryos from nc 10–14, color-coded by stage ($n = 56$). The top 15% of Dorsal nuclear levels at each nuclear cycle is shown in the inset. (*B*) Box-and-whisker plot of Dorsal levels in ventral-most nuclei correspond to the peak amplitude at each nuclear cycle (blue). Basal levels represent Dorsal levels in lateral and dorsal regions of the embryo outside of the graded distribution of Dorsal (orange). Median intensity is shown as a horizontal bar in the box; box denotes data bounded by interquartile range. Whiskers show the distribution of data. Asterisks denote outliers. (*Inset*) Cartoon of Amplitude and Basal portion of signal. (*C*) When the peaks of each of the curves in *A* are normalized to 1, all curves fall along the same Gaussian curve with minor variation in curve width. (*D*) Box-and-whisker plots show Dorsal nuclear gradient widths remain constant throughout embryogenesis. (*Inset*) Width parameters correspond to 2× width of best-fit curve at 60% maximal. For nc 10–14, $n = 7, 3, 3, 7$, and 35, respectively.

(*SI Text*, section 13), and thus cannot be attributed to technical noise. Considering our results thus far—that the levels of nuclear Dorsal are highly dynamic, the gradient widths remain constant, and yet putative Dorsal target genes such as *ind*, *brk*, and *sog* exhibit boundaries of expression in regions where the levels of Dorsal are unchanging—we questioned how Dorsal could supply the positional information necessary to pattern the entire DV axis.

To investigate the relationship between Dorsal nuclear concentration and gene expression outputs, we quantified Dorsal in embryos from either $Toll^{rm9}/Toll^{rm10}$ or $Toll^{10B}$ mothers, both of which lack a wt Dorsal gradient. In $Toll^{rm9}/Toll^{rm10}$ mutants, we observed uniform, low levels of nuclear Dorsal, with wide variation in concentration from embryo-to-embryo (Fig. 4*E*) (17). In these mutants, *ind* and *vnd* gene expression is observed in stripes along the anterior-posterior (AP) axis in variable domains (Fig. 4 *C* and *D*), as has been previously noted (18). These expression domains were explained by assuming that *vnd* is seen in a broad domain in embryos with higher amounts of Dorsal than embryos which express *ind* broadly (19). However, we find that *vnd* expression is broadly expressed only at early time points and the majority of cellularized embryos express both genes, with a ring of *vnd* present at roughly 70% egg length (Fig. 4 *C* and *D*). The expression of *ind* and *vnd* in the same embryo is unexpected as these genes were previously considered to be distinct Dorsal threshold outputs (18). In $Toll^{10B}$ mutants, the Toll receptor is constitutively active throughout the embryo, and only mesoderm cell fates result, suggesting that Dorsal nuclear levels are high and uniform in these embryos, or have at best an extremely shallow gradient (13). We measured nuclear Dorsal in these embryos and found Dorsal levels were also variable, and higher on average than observed in $Toll^{rm9}/Toll^{rm10}$ mutant embryos, yet with some overlap (Fig. 4*E*). Despite this overlap, the Dorsal nuclear levels are statistically distinct from those in $Toll^{rm9}/Toll^{rm10}$ embryos (see *SI Text*, section 13). In accordance with this, all of the $Toll^{10B}$ embryos express *snail* to the exclusion of *vnd* or *ind* (Fig. 4*B*).

Given that Dorsal levels can vary widely while still producing reliable gene expression, we tested the relationship between *dorsal* gene dosage and gene expression outputs by examining embryos with different copies of maternal *dorsal*. In heterozygous embryos ($dl^1/+$), a simple model would predict half the amount of Dorsal in the embryo. However, in these embryos, the Dorsal gradient is flattened in ventral regions, rather than bell-shaped as in wt, but the steepness is retained in ventral-lateral regions (Fig. 5 *B* and *D*). This result was also observed using other *dorsal* alleles (*SI Text*, section 11). We measured the expression domain of *sog* in these embryos and found it to be indistinguishable from wt (Fig. 5*B* and *SI Text*, sections 10 and 13). This corresponds to the observation that, in ventral-lateral regions, where gene expression boundaries (such as those between *sna* and *sog*) are delineated, the Dorsal gradient retains a steepness similar to that found in wt (*SI Text*, section 13).

We also imaged embryos carrying a copy of transgenic *dorsal-gfp* (3). We found the Dorsal gradients in these embryos retained their Gaussian shape, yet were significantly wider than wt and reached higher amplitudes (Fig. 5 and *SI Text*, sections 12 and 13). Additionally, the *sog* domain is significantly widened in these

DEVELOPMENTAL BIOLOGY

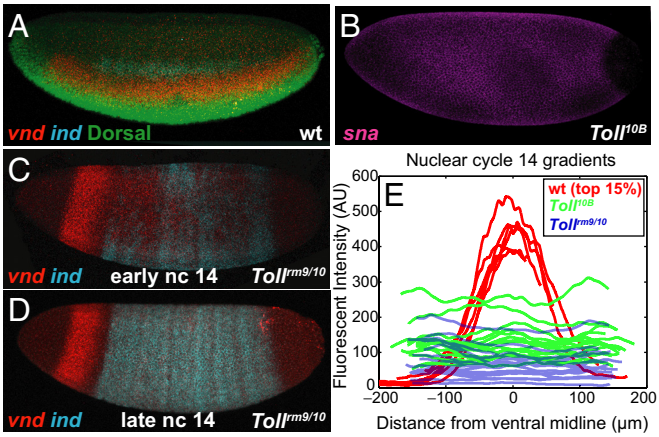

Fig. 4. Dorsal nuclear localization in wt and mutant embryos reveals a wide range of nuclear concentrations. Dual fluorescent in situ and antibody staining: *vnd*, *ind*, and/or *sna* riboprobes and anti-Dorsal antibody were used. (*A*) Dorsal nuclear localization in wt (green) with wt expression domains of *vnd* (red) and *ind* (blue) transcripts. (*B*) *sna* expression (purple) in *Toll10b* mutant embryos is ubiquitous except for repression in posterior of the embryo. (*C* and *D*) *Tollrm9/Tollrm10* mutant embryos with variable expression of *ind* (blue) and *vnd* (red) transcripts. A temporal change in the patterns is observed: (*C*) early nc 14, and (*D*) late nc 14. (*E*) Nuclear localization of Dorsal in nc 14 embryos of $Toll^{10B}$ mutants (n = 15) (green) and $Toll^{rm9}/Toll^{rm10}$ mutants (n = 17) (blue) and the top 15% of all nc 14 wt embryos (n = 6) (red).

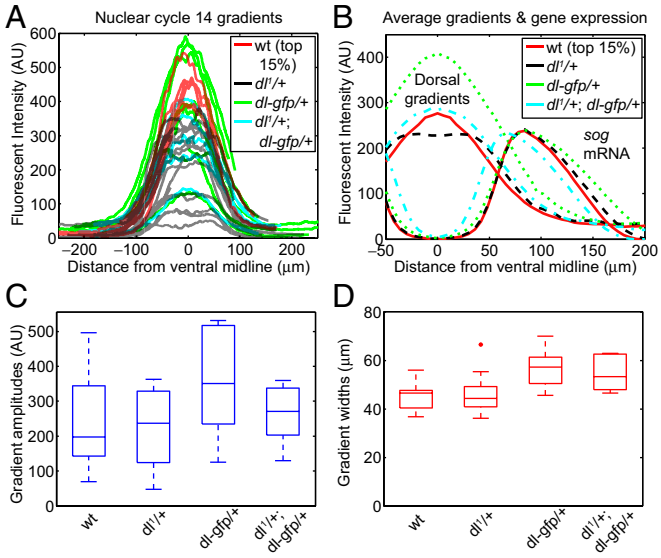

Fig. 5. Mutant embryos with genetically manipulated Dorsal produce similar gene expression outputs. (*A*) dl^1/+ heterozygous embryos (black) have a flattened plateau of Dorsal concentration instead of the peak in ventral regions seen in wt embryos, top 15% of nc 14 (n = 6) (red). *dl-gfp* embryos contain an additional copy of *dorsal* and have significantly wider and higher Dorsal gradients (green). dl^1/+; *dl-gfp*/+ embryos (cyan) are wider than wt, yet not higher. (*B*) Average nc 14 Dorsal gradients from wt (solid red), dl^1/+ (dashed black, n = 16), *dl-gfp*/+ embryos (dotted green, n = 8), and dl^1/+; *dl-gfp*/+ embryos (dot-dashed cyan, n = 5). From these average gradients, the trends from *A* are clearly seen. Furthermore, note that gradients from wt and dl^1/+ embryos have close overlap in ventral-lateral regions. Also shown: *sog* mRNA expression patterns. While *sog* expression in dl^1/+ and dl^1/+; *dl-gfp*/+ embryos is indistinguishable from wt, *dl-gfp*/+ embryos exhibit a widened expression domain extending into more dorsal regions of the embryo (*SI Text*, section 13). (*C* and *D*) Box plots of gradient amplitudes (*C*) and widths (*D*) of each of the genotypes described here.

embryos. The changes in the Dorsal nuclear gradient may be caused by an extra gene dose of *dorsal*. To address this, we analyzed embryos from dl^1/+; *dl-gfp*/+ mothers and found that, while these embryos have gradient amplitudes similar to wt, the widths were expanded (Fig. 5 *B–D* and *SI Text*, section 13); and while the average *sog* domain appears to be ventralized in these embryos (Fig. 5*B*), it is statistically indistinguishable from wt embryos (*SI Text*, section 13). We conclude that the widened gradient is a specific result of the *dl-gfp* transgene and not simply due to an additional copy of *dorsal* (see *Discussion*, Fig. 5, and *SI Text*, section 14).

Discussion

In this study, we used whole mount staining and quantitative imaging to analyze the relationship between the amount of nuclear Dorsal and the gene expression outputs Dorsal regulates. Surprisingly, we found that intermediate regions of the embryo, where *ind* and the dorsal portion of *sog* are expressed, are consistently beyond the range of graded nuclear Dorsal (Fig. 2). While small amounts of Dorsal are present in these nuclei, these basal levels are also present in the dorsal-most nuclei and thus cannot supply additional positional information. In light of this, we were particularly curious how the borders of these genes were reliably positioned. One possibility is that the Dorsal gradient is initially broader and then narrows as seen in the short germ beetle, *Tribolium castaneum* (20, 21). However, our results dismiss this possibility by showing that there is little to no change in either the Gaussian shape or the extent of the Dorsal gradient during nc 10–14 (Fig. 3).

Alternatively, gene expression in intermediate regions could be activated or refined by the combinatorial action of other factors. For example, an unknown dorsally localized factor acts to establish the dorsal border of *ind* (Fig. 6*A*) (22). Furthermore, genetic evidence implies EGFR participates in *ind* up-regulation, consistent with the late onset of *ind* expression (23, 24). Thus, combinatorial interactions requiring EGFR could be responsible for *ind* expression and the maintenance of *sog* and *brk* expression following cellularization (Fig. 6*A*). Notably, our data also suggest that Dorsal-mediated repression alone cannot account for the patterns of dorsal ectoderm genes such as *dpp*, *zen*, and *tld*. It is known that the repressor Brinker restricts these genes to the dorsal half of the embryo, but only at cellularization (25). Further studies will be necessary to determine how positional information is initially supplied to the intermediate regions of the embryo, as we suggest that other unidentified factors function with Dorsal in precellularized embryos to demarcate the boundaries of these expression domains.

Although the shape and width of the wt Dorsal gradient is constant in time, our data show that the overall levels of nuclear Dorsal at any given DV axis location vary widely from embryo-to-embryo. We propose that this variability is the result of observing snapshots of a rapid, time-dependent process in which net nuclear import of Dorsal during interphase causes an increase in Dorsal levels within nuclei, followed by rapid export during mitosis when nuclear envelopes break down. This phenomenon was also observed previously in single-nucleus time lapses using a Dorsal-GFP fusion protein (3).

Despite the rapid dynamics of measured nuclear Dorsal levels, the gene expression boundaries of Dorsal target genes along the DV axis remain surprisingly robust. To explain this, we favor a model in which threshold levels of Dorsal activate transcription of mRNA in real time, following the dynamics of nuclear Dorsal levels (Fig. 6*B*). In this model, mRNA levels increase when Dorsal levels surpass a given threshold, and decline (due to degradation) when Dorsal levels are subthreshold. While this mechanism alone could result in fuzzy gene expression domains, combinatorial interactions with other transcription factors at regulatory elements are capable of restoring sharp boundaries.

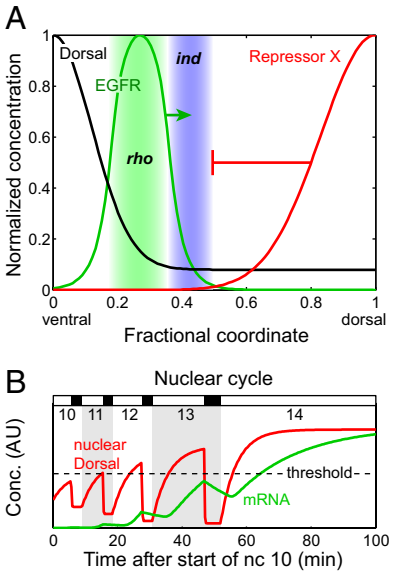

Fig. 6. Proposed mechanism of Dorsal-mediated patterning. (*A*) A combinatorial model for DV patterning. Dorsal and EGFR may function together to specify *ind*, and other genes, in the presumptive neurogenic ectoderm. Additionally, repression by an unknown factor (X) may serve to limit the dorsal-extent of these genes. (*B*) Gene expression in the midst of dynamic Dorsal nuclear concentration. Dorsal levels fluctuate during and between nuclear cycles (red curve). When Dorsal surpasses a minimally sufficient level (dashed line) of protein in the nucleus, and the requisite additional factors are present, transcription of a given target gene occurs. Transcripts (green curve) accumulate during the time when Dorsal is above a given threshold and then diminish when Dorsal falls below that threshold. The bar at the top of the simulated plot demarcates interphase (white) and mitosis (black).

This "pre-steady-state decoding" of the Dorsal gradient has also been suggested for the Bicoid gradient (26).

These dynamics of Dorsal nuclear levels are not restricted to wt embryos, but were observed in all embryos studied, including those with relatively uniform Dorsal levels (from $Toll^{rm9}/Toll^{rm10}$ and $Toll^{10B}$ mothers). Surprisingly, in the $Toll^{rm9}/Toll^{rm10}$ background, both *ind* and *vnd* were frequently seen within the same embryo, yet in spatially distinct locations (Fig. 4 *C* and *D*). One scenario for this result is that Dorsal levels are higher toward the anterior of the embryo, resulting in a ring of *vnd* expression at roughly 70% egg length. However, we found that AP modulation of Dorsal levels does not explain the observed pattern (*SI Text*, section 9). We cannot completely rule out a temporal dependence to this expression; perhaps higher levels of Dorsal turn on *vnd* at an earlier stage. However, this would not explain the progression of early, broadly expressed *vnd*, replaced later by *ind*. Alternatively, direct activation of *ind* by EGFR could explain this phenotype, as ubiquitous *rho* expression seen in $Toll^{rm9}/Toll^{rm10}$ embryos would cause heightened EGFR signaling, perhaps enough to overcome repression of *ind* by Vnd (24). However, this does not explain the AP asymmetry. Previous studies on an allelic series of *dorsal* revealed extra sensitivity at 70% egg length (10), while others have directly shown that AP factors influence expression along the DV axis and bind to the regulatory regions of DV genes (19, 27, 28). These AP factors may also function to regulate gene expression in this background.

It is evident that the levels of nuclear Dorsal measured in mutants in this work are much lower than maximal levels found in wt embryos (Fig. 4*E*). Therefore, in light of a recent study of Bicoid-dependent patterning along the AP axis of *Drosophila* embryos (29), it may be tempting to ask whether the levels of nuclear Dorsal measured in $Toll^{rm9}/Toll^{rm10}$ or $Toll^{10B}$ embryos correspond to those found in the *vnd* or *sna* domains, respectively, of wild type embryos. If the Dorsal gradient were at steady state, signaling levels should either be above a given threshold, resulting in the presence of mRNA, or below it, resulting in lack of mRNA. While the Bicoid nuclear gradient appears to achieve a stable distribution quickly (16), our data reveal the Dorsal gradient to be dynamic through cellularization. Considering these dynamics, we must ask instead at what time points during development does signaling from Dorsal and the necessary co-factors exceed a threshold to regulate gene transcription, and whether over time this would lead to an accumulation of mRNA in the expected patterns (Fig. 6*B*).

Finally, to test the dosage dependence of Dorsal on gene expression, we examined embryos with either one or three copies of maternally supplied Dorsal. We noted that, in the heterozygous embryos ($dl^1/+$), the overall shape of the Dorsal gradient was not retained. Instead of a smooth Gaussian peak, Dorsal nuclear localization formed a plateau. Despite this altered shape, or perhaps because of it, gene expression outputs remain virtually unchanged from wt. When gene dosage is low, it appears that compensatory mechanisms exist to maintain graded Dorsal in the region of the embryo where it is presumably important (i.e., presumptive neurogenic ectoderm), which may explain previously observed synergistic genetic interactions between *dorsal*, *snail*, and *twist* (30). The distribution of nuclear Dorsal in this region is very similar to wt (Fig. 5*B*). While it is not immediately clear what form of regulation could be responsible for the redistribution of nuclear Dorsal, we propose it could be dependent on feedback involving zygotic gene expression. In contrast, embryos carrying a copy of *dl-gfp* have significantly wider and higher-amplitude gradients, and gene expression in these embryos is shifted dorsally (Fig. 5 *B–D*). The expanded widths of these gradients cannot be explained by a higher gene dose of *dl*, as embryos from mothers carrying this transgene, in a heterozygous background, also have expanded gradients (Fig. 5 *B* and *D*). This is consistent with the nature of the *dl-gfp* transgene, which lacks a putative export sequence, and may explain its failure to complement *dl*-null mutants (see *SI Text*, section 14).

Our results are consistent with previous studies that the levels of Dorsal in ventral and ventral-lateral regions regulate differential gene expression, but leave open the question of how dorsal-lateral and dorsal regions of the embryo are patterned. Furthermore, the observed dynamics of the Dorsal gradient are difficult to reconcile with the classical morphogen gradient model. Instead, our data support the view that information provided by Dorsal is accumulated over time (Fig. 6*B*) as well as augmented by interactions with other transcription factors that function to regulate gene expression along the DV axis (Fig. 6*A*) (8–10, 31, 32). In total, our data support a model in which Dorsal provides crucial, yet constantly changing positional information to the embryo, while combinatorial interactions between transcription factors at regulatory sites establish sharp, precise boundaries of gene expression.

Materials and Methods

Fly Lines. *yw* flies were used to quantify the wt Dorsal gradient. Dorsal mutant heterozygous and homozygous mothers were generated using dl^1 cn^1 sca^1/*CyO I* (2)*DTS100*^{1}, or dl^4 pr^1 cn^1 wx^{wxt} bw^1/*CyO*, both from the Bloomington Stock Center, or dl^8 *b pr cn wxt bw*/*CyO* from R. Steward, Rutgers University. The generation of $Toll^{rm9}/Toll^{rm10}$ and $Toll^{10B}$ mutant embryos has been previously described (17). *dl-gfp* flies were obtained from R. Steward (3).

Antibody Staining and Fluorescent in Situ Hybridization (FISH). Dual fluorescent in situ and antibody staining were performed using established methods omitting the Proteinase K procedure (33). Antisense RNA probes and Alexa Fluor 647 anti Sheep secondary (Invitrogen 21448) were used to visualize RNA localization of target gene expression. α-Dorsal 7A4 monoclonal antibody (DSHB) and Alexa Fluor 488 α-mouse secondary (Invitrogen A21202) were used to detect Dorsal protein localization. α-Histone H3 polyclonal rabbit antibody (Abcam #ab1791–100) and Alexa Fluor 555 anti-rabbit secondary (Invitrogen

A31572) were used to detect Histones and served as a nuclear marker. Mutant and wt embryos were stained during the same experiment. wt embryos were added to each of the mutant embryo tubes as staining controls for all of the experiments except the *dl-gfp*, $dl^1/+$, and $dl^1/+$;*dl-gfp*/+ lines, because these genotypes could not be visually distinguished from wt.

Image Acquisition and Processing. The LSM 5 Pascal (Zeiss) microscope was used to acquire confocal *z*-stacks of fixed and labeled embryos. Briefly, confocal stacks were acquired to image through at least 50% of the embryo, and flat-field correction applied. For groups of *y*–*z* sections, the location of the periphery of the embryo was found computationally. We then used a keystone transformation to computationally ''unroll'' the embryo's peripheral shell slice by slice. This unrolled shell was then averaged in the proximal-distal direction. This exchanges a 3D data set for a smaller, more easily manipulated 2D sheet (see *SI Text*).

Dorsal Protein Quantification. Dorsal was quantified in embryos in nc 10–14. Starting from the 2D sheet representation of the 3D data set, the nuclei were segmented using standard protocols in Matlab (see *SI Text*). Up to an additive constant, the Dorsal concentration in each nucleus was calculated to be proportional to the intensity of the Dorsal image in the location of the nucleus normalized by the intensity of the same nucleus in the Histone H3 image (for depth correction):

$$c_{dl,i} \propto I_{dl,i}/I_{hist,i} + k,$$

where $I_{dl,i}$ and $I_{hist,i}$ are the intensities of the ith nucleus in the Dorsal and Histone images, respectively, and k is a constant describing non-specific antibody binding. We estimate the value of k by imaging embryos derived from dl^1 mothers.

The Dorsal nuclear gradients were fit to Gaussian-shaped curves to determine the following global properties of the gradient: amplitude, basal levels, presumptive location of ventral midline, and length scale of decay (width):

$$c_{dl} = A \exp(-(x - \mu)^2/(2\sigma^2)) + B,$$

where A and B denote the amplitude and basal levels of the fitted Dorsal gradient, respectively, μ denotes the location of the presumptive ventral midline, and σ is the length scale, or width, of the gradient. For each imaged Dorsal gradient, the values of these parameters were optimized in the least squares sense. Because signal decay was problematic at the edges of the image, only the central 60% of the image (along the AP axis) was used in the optimization.

ACKNOWLEDGMENTS. We thank Scott Fraser for helpful discussions regarding the imaging procedures and R. Steward for sharing fly stocks. This work was supported by Grant GM077668 (to A.S.). G.T.R. is a fellow of The Jane Coffin Childs Memorial Fund for Medical Research and was supported by a grant from The Jane Coffin Childs Memorial Fund for Medical Research.

1. Ashe HL, Briscoe J (2006) The interpretation of morphogen gradients. *Development* 133:385–394.
2. Moussian B, Roth S (2005) Dorsoventral axis formation in the *Drosophila* embryo–shaping and transducing a morphogen gradient. *Curr Biol* 15:R887–899.
3. DeLotto R, DeLotto Y, Steward R, Lippincott-Schwartz J (2007) Nucleocytoplasmic shuttling mediates the dynamic maintenance of nuclear Dorsal levels during *Drosophila* embryogenesis. *Development* 134:4233–4241.
4. Reeves GT, Stathopoulos A (2009) in *Cold Spring Harbor Perspectives in Biology*, eds Briscoe J, Lawrence P, Vincent J.-P. (Cold Spring Harbor Lab Press, Plainview, NY).
5. Ip YT, Kraut R, Levine M, Rushlow CA (1991) The dorsal morphogen is a sequence-specific DNA-binding protein that interacts with a long-range repression element in *Drosophila*. *Cell* 64:439–446.
6. Jiang J, Levine M (1993) Binding affinities and cooperative interactions with bHLH activators delimit threshold responses to the dorsal gradient morphogen. *Cell* 72:741–752.
7. Papatsenko D, Levine M (2005) Quantitative analysis of binding motifs mediating diverse spatial readouts of the Dorsal gradient in the *Drosophila* embryo. *Proc Natl Acad Sci USA* 102:4966–4971.
8. Liberman LM, Stathopoulos A (2008) Design flexibility in cis-regulatory control of gene expression: Synthetic and comparative evidence. *Dev Biol* 327:578–589.
9. Ip YT, Park RE, Kosman D, Yazdanbakhsh K, Levine M (1992) Dorsal–Twist interactions establish snail expression in the presumptive mesoderm of the *Drosophila* embryo. *Genes Dev* 6:1518–1530.
10. González-Crespo S, Levine M (1993) Interactions between dorsal and helix–loop–helix proteins initiate the differentiation of the embryonic mesoderm and neuroectoderm in *Drosophila*. *Genes Dev* 7:1703–1713.
11. Zinzen R, Senger K, Levine M, Papatsenko D (2006) Computational models for neurogenic gene expression in the *Drosophila* embryo. *Curr Biol* 16:1358–1365.
12. Luengo Hendriks CL, et al. (2006) Three-dimensional morphology and gene expression in the *Drosophila* blastoderm at cellular resolution I: Data acquisition pipeline. *Genome Biol* 7:R123.
13. Roth S, Stein D, Nüsslein-Volhard C (1989) A gradient of nuclear localization of the dorsal protein determines dorsoventral pattern in the *Drosophila* embryo. *Cell* 59:1189–1202.
14. Rushlow CA, Han K, Manley JL, Levine M (1989) The graded distribution of the dorsal morphogen is initiated by selective nuclear transport in *Drosophila*. *Cell* 59:1165–1177.
15. Steward R, Zusman SB, Huang LH, Schedl P (1988) The dorsal protein is distributed in a gradient in early *Drosophila* embryos. *Cell* 55:487–495.
16. Gregor T, Wieschaus EF, McGregor AP, Bialek W, Tank DW (2007) Stability and nuclear dynamics of the bicoid morphogen gradient. *Cell* 130:141–152.
17. Stathopoulos A, Van Drenth M, Erives A, Markstein M, Levine M (2002) Whole-genome analysis of dorsal-ventral patterning in the *Drosophila* embryo. *Cell* 111:687–701.
18. Cowden J, Levine M (2003) Ventral dominance governs sequential patterns of gene expression across the dorsal-ventral axis of the neuroectoderm in the *Drosophila* embryo. *Dev Biol* 262:335–349.
19. Mizutani CM, Meyer N, Roelink H, Bier E (2006) Threshold-dependent BMP-mediated repression: A model for a conserved mechanism that patterns the neuroectoderm. *PLoS Biol* 4:e313.
20. Chen G, Handel K, Roth S (2000) The maternal NF-kappaB/dorsal gradient of Tribolium castaneum: Dynamics of early dorsoventral patterning in a short-germ beetle. *Development* 127:5145–5156.
21. Nunes da Fonseca R, et al. (2008) Self-regulatory circuits in dorsoventral axis formation of the short-germ beetle *Tribolium castaneum*. *Dev Cell* 14:605–615.
22. Stathopoulos A, Levine M (2005) Localized repressors delineate the neurogenic ectoderm in the early *Drosophila* embryo. *Dev Biol* 280:482.
23. Hong JW, Hendrix DA, Papatsenko D, Levine MS (2008) How the Dorsal gradient works: Insights from postgenome technologies. *Proc Natl Acad Sci USA* 105:20072–20076.
24. Von Ohlen T, Doe CQ (2000) Convergence of dorsal, dpp, and egfr signaling pathways subdivides the *Drosophila* neuroectoderm into three dorsal-ventral columns. *Dev Biol* 224:362–372.
25. Jaźwińska A, Rushlow C, Roth S (1999) The role of brinker in mediating the graded response to Dpp in early *Drosophila* embryos. *Development* 126:3323–3334.
26. Bergmann S, et al. (2007) Pre-steady-state decoding of the Bicoid morphogen gradient. *PLoS Biol* 5:e46.
27. Zeitlinger J, et al. (2007) Whole-genome ChIP-chip analysis of Dorsal, Twist, and Snail suggests integration of diverse patterning processes in the *Drosophila* embryo. *Genes Dev* 21:385–390.
28. Li XY, et al. (2008) Transcription factors bind thousands of active and inactive regions in the *Drosophila* blastoderm. *PLoS Biol* 6:e27.
29. Ochoa-Espinosa A, Yu D, Tsirigos A, Struffi P, Small S (2009) Sackler Special Feature: Anterior–posterior positional information in the absence of a strong Bicoid gradient. *Proc Natl Acad Sci USA* 106:3823–3828.
30. Simpson P (1983) Maternal-zygotic gene interactions during formation of the dorsoventral pattern in *Drosophila* embryos. *Genetics* 105:615–632.
31. Senger K, et al. (2004) Immunity regulatory DNAs share common organizational features in *Drosophila*. *Mol Cell* 13:19–32.
32. Stathopoulos A, Levine M (2002) Linear signaling in the Toll-Dorsal pathway of *Drosophila*: Activated Pelle kinase specifies all threshold outputs of gene expression while the bHLH protein Twist specifies a subset. *Development* 129:3411–3419.
33. Kosman D, et al. (2004) Multiplex detection of RNA expression in *Drosophila* embryos. *Science* 305:846.